

# Intermetallic PtPb Nanoparticles Prepared by Sodium Naphthalide Reduction of Metal-Organic Precursors: Electrocatalytic Oxidation of Formic Acid

Laif R. Alden, Daniel K. Han, Futoshi Matsumoto, Héctor D. Abruña, and Francis J. DiSalvo\*

Department of Chemistry and Chemical Biology, Baker Laboratory, Cornell University, Ithaca, New York 14853

Received April 21, 2006. Revised Manuscript Received July 7, 2006

Intermetallic PtPb nanoparticles have been synthesized by the chemical reduction of dimethyl(1,5-cyclooctadiene)platinum and lead(II) 2-ethylhexanoate by sodium naphthalide in THF or diglyme. If exposed to air quickly, the product becomes warm to the touch presumably due to surface oxidation, yet powder X-ray diffraction shows that the product is crystalline PtPb with a mean crystal domain size of 16 nm. If the product is exposed to air slowly, the pXRD pattern shows much broader and weaker peaks. Performing the synthesis in diglyme allows the crystal domain size to be controlled by annealing at temperatures below the boiling point of diglyme (162 °C). The product has been characterized by SEM, STEM, CBED, and EDX. Activity of the PtPb nanoparticles for formic acid oxidation is reported. The samples evaluated exhibit a remarkable ability to oxidize formic acid, with high mass activities and onset potentials similar to those reported previously for bulk PtPb electrodes.

## Introduction

While methods to produce metallic nanoparticles containing more than one element have been reported, the majority of this work has been focused on combinations of metals that form alloys.<sup>1–3</sup> In crystalline alloys (also known as random solid solutions), the positions of the atomic sites are ordered and periodic, but the site occupancy can only be described probabilistically and is determined by the stoichiometric ratio of the elements that are alloyed. On the other hand, different crystallographic positions in prototypical ordered intermetallic compounds (intermetallics) are occupied by only one element, leading to compositional as well as positional order.<sup>4</sup> As a general rule, elements of similar size, electronegativity, etc., will tend to form random solid solutions (alloys), while elements that are more dissimilar tend to form intermetallics.<sup>5,6</sup> Some intermetallic nanoparticles have been previously synthesized using various synthetic techniques including aluminum-based intermetallics<sup>7–11</sup> and noble metal-based intermetallics.<sup>12–18</sup>

The reduction of metal cations in solution is a common way to prepare metallic nanoparticles.<sup>1–3</sup> One of the synthetic challenges in preparing homogeneous nanoparticles of intermetallics lies in the fact that elements which form intermetallics can have very different rates of reduction. The dissimilar elements must be co-reduced simultaneously to form a homogeneous product. If one element is reduced faster than the other, the product may have core/shell-like morphologies (one element coating the other) or mixtures of separate particles each containing only one element. In general, as the differences in the rate of reduction of the different metals increases, co-reduction becomes more difficult. This additional challenge plus others typically associated with the preparation of metallic nanoparticles in general (e.g., prevention of agglomeration) may be why comparatively few reports of ordered intermetallic nanoparticles have been reported to date.

To avoid these problems, reducing agents and precursors must be chosen so that the rate of reduction is nearly diffusion-limited. That is, the reduction rate should be

- (1) Roucoux, A.; Schulz, J.; Patin, H. *Chem. Rev.* **2002**, *102*, 3757–3778.
- (2) Cushing, B. L.; Kolesnichenko, V. L.; O'Connor, C. J. *Chem. Rev.* **2004**, *10*, 3893–3946.
- (3) Bönnemann, H.; Richards, R. M. *Eur. J. Inorg. Chem.* **2001**, 2455–2480.
- (4) West, A. R. *Basic Solid State Chemistry*, 2nd ed.; John Wiley and Sons: New York, 1999.
- (5) Villars, P. *J. Less-Common Met.* **1983**, *92*, 215–238.
- (6) Villars, P.; Brandenburg, K.; Berndt, M.; LeClair, S.; Jackson, A.; Pao, Y.-H.; Igel'nik, B.; Oxley, M.; Bakshi, B.; Chen, P.; Iwata, S. *J. Alloys Compd.* **2001**, *317–318*, 26–38.
- (7) Ma, J.; Du, Y. *JAC* **2005**, *395*, 277–279.
- (8) Liu, T.; Shao, H.; Li, X. *Nanotechnology* **2003**, *14*, 542–545.
- (9) Haber, J. A.; Gunda, N. V.; Balbach, J. J.; Conradi, M. S.; Buhro, W. E. *Chem. Mater.* **2000**, *12*, 973–982.
- (10) Haber, J. A.; Crane, J. L.; Buhro, W. E.; Fray, C. A.; Sasty, S. M. L.; Balbach, J. L.; Conradi, M. S. *Adv. Mater.* **1996**, *8*, 163–166.

- (11) Buhro, W. E.; Haber, J. A.; Waller, B. E.; Trentler, T. J.; Suryanarayanan, R.; Frey, C. A.; Sasty, S. M. L. *Polym. Mater. Sci. Eng.* **1995**, *73*, 39–40.
- (12) Bönnemann, H.; Britz, P.; Vogel, W. *Langmuir* **1998**, *14*, 6654–6657.
- (13) Ould-Ely, T.; Thurston, J. H.; Kumar, A.; Respaud, M.; Guo, W.; Weidenthaler, C.; Whitmir, K. H. *Chem. Mater.* **2005**, *17*, 4750–4754.
- (14) Schaak, R. E.; Sra, A. K.; Leonard, B. M.; Cable, R. E.; Bauer, J. C.; Han, Y.-F.; Means, J.; Teizer, W.; Vasquez, Y.; Funck, E. S. *J. Am. Chem. Soc.* **2005**, *127*, 3506–3515.
- (15) Sra, A. K.; Ewers, T. D.; Schaak, R. E. *Chem. Mater.* **2005**, *17*, 758–766.
- (16) Sra, A. K.; Schaak, R. E. *J. Am. Chem. Soc.* **2004**, *126*, 6667–6672.
- (17) Cable, R. E.; Schaak, R. E. *Chem. Mater.* **2005**, *17*, 6835–6841.
- (18) Roychowdhury, C.; Matsumoto, F.; Mutolo, P. F.; Abruña, H. D.; DiSalvo, F. J. *Chem. Mater.* **2005**, *17*, 5871–6876.

determined primarily by the rate of mixing of the reactants, not by other factors, such as electron-transfer rates. Finally, all precursors must be compatible with each other and soluble in a suitable solvent. Both the reducing agent and the products must be stable in the same solvent as well.

This research was motivated by recent work exploring the electrocatalytic behavior of several platinum-based intermetallics, specifically to investigate their potential as electrocatalysts in fuel cells.<sup>19,20</sup> Currently, platinum-based alloy catalysts do not meet the performance goals necessary for fuel cell applications.<sup>21–24</sup> Electrochemical testing of some platinum-based intermetallics in bulk shows much promise. PtPb in particular has been shown to exhibit remarkable electrocatalytic activity for the oxidation of formic acid.<sup>19</sup> However, it is clear that these compounds must be available as high surface area nanoparticles if they are to be used in real working fuel cell applications. For instance, in some technologies, Pt nanoparticles in the 3–5 nm diameter range show optimal performance per unit mass. However, we are continuing to search for even more active catalysts, especially for other potential fuels. Thus, we need to develop generic techniques that could allow the preparation of nanoparticles of many different intermetallic compounds. Here, we report the synthesis of PtPb nanoparticles, prepared by reducing metal-organic precursors with sodium naphthalide. Sodium naphthalide was chosen for this work because it is a strong reducing agent that potentially could be used with a wide variety of precursors of different metals. In fact, sodium naphthalide has been used previously to prepare nanoparticles of more electropositive single elements.<sup>25–27</sup> The electrocatalytic ability of these nanoparticles to oxidize formic acid is also reported. The synthesis of PtPb nanoparticles has been reported previously by another process,<sup>17</sup> but electrocatalytic activity was not investigated.

## Experimental Section

**Materials.** All chemicals except lead(II) 2-ethylhexanoate were used as received. Sodium metal and all solvents were purchased from Aldrich. Naphthalene was purchased from Fisher. Dimethyl-(1,5-cyclooctadiene)platinum and lead(II) 2-ethylhexanoate were purchased from STREM Chemicals Inc. Because of the high viscosity of lead(II) 2-ethylhexanoate, 0.05 M stock solutions were prepared by dissolving 2.496 g in 100 mL of tetrahydrofuran (THF). All solvents (except for ethanol) were freshly distilled over sodium prior to use.

**Sodium Naphthalide.** Sodium naphthalide solutions were prepared in either THF or diglyme (diethylene glycol dimethyl ether) according to well-known literature methods.<sup>28</sup> Stoichiometric amounts of naphthalene (0.1923 g, 1.5 mmol) and sodium metal (0.0345 g, 1.5 mmol) were weighed out in an argon atmosphere glovebox and added to a flask containing 40 mL of solvent. The sealed flask was removed from the glovebox and stirred overnight under argon to produce a dark green sodium naphthalide solution.

**PtPb Nanoparticles.** In a typical reaction, 0.0833 g of dimethyl-(1,5-cyclooctadiene)platinum (0.25 mmol) was dissolved in a 5 mL aliquot of a 0.05 M stock solution of lead(II) 2-ethylhexanoate in (0.25 mmol of lead(II) 2-ethylhexanoate). This solution was injected into a flask containing a freshly prepared sodium naphthalide solution (40 mL, 0.0375 M, 1.5 mmol—a 50% excess over the 1.0 mmol needed to fully reduce the Pt<sup>2+</sup> and Pb<sup>2+</sup>). The dark green solution immediately became black and opaque. In experiments where THF was the solvent, the flask was stirred for 10 min. In experiments where diglyme was the solvent, the flask was immediately immersed in an oil bath and heated to a specified temperature for a specified amount of time (see Results below), after which it was allowed to cool to 40 °C. In both THF and diglyme experiments, the solvent and any volatile side products were carefully pumped out of the flask, using first static vacuum followed by dynamic vacuum, leaving a black residue. Once the flask was pumped down to a suitably low pressure (~200 mTorr), 40 mL of hexanes were distilled and the sealed flask was sonicated in an immersion bath sonicator for 10 min. The contents of the flask were then transferred to a centrifuge tube with a cannula and centrifuged (2000 rpm, 10 min). The supernatant was removed with a syringe, 40 mL of degassed absolute ethanol was added to the black precipitate, and the tube was sonicated for 10 min and centrifuged again. This supernatant was also removed with a syringe and the black precipitate was dried under vacuum. In the initial experiments where THF was the solvent, the product was exposed to air by breaking the seal of the evacuated tube, resulting in the black precipitate giving off a small plume of white smoke and the tube becoming warm to the touch. In later experiments (using both THF and diglyme), the tube was backfilled with argon before breaking the seal. The tube was then allowed to stand undisturbed overnight so as to allow air to diffuse into the tube slowly.

**Instrumentation.** The sonicator used was a model 3150 Bransonic ultrasonic cleaner. All powder X-ray diffraction scans were taken on a Scintag XDS 200 powder X-ray diffractometer. pXRD patterns taken under inert conditions were prepared by loading the sample into the sample holder and covering it with a mylar film in an argon-filled glovebox before the pXRD pattern was taken. Images from a scanning electron microscope (SEM) were taken on a LEO-1550 field emission SEM. All ultra-high vacuum scanning transmission electron microscope (STEM) and convergent beam electron diffraction (CBED) images as well as all energy dispersive X-ray analysis (EDX) data were taken on a VG HB01UX UHV STEM. Specimens were prepared for electron microscopy by ultrasonically 5 mg of nanoparticles (Microson XL2000 Ultrasonic Homogenizer/Cell Disruptor) in 5 mL of isopropanol for 5 min to obtain a dark gray suspension. For SEM, 2 drops of each of the dispersions were pipetted onto a clean aluminum stub and dried. For STEM, an ultrathin TEM grid was dipped in the suspension and dried.

**Electrocatalytic Activity.** The procedure used here for determining the electrocatalytic activity of intermetallic nanoparticles has been reported previously.<sup>18</sup> In this case, the electrocatalytic suspensions (2.5–5 mg of catalyst, 3.98 mL of distilled water, 1 mL of

- (19) Casado-Rivera, E.; Volpe, D. J.; Alden, L.; Lind, C.; Downie, C.; Vázquez-Alvarez, T.; Angelo, A. C. D.; DiSalvo, F. J.; Abruña, H. D. *J. Am. Chem. Soc.* **2004**, *126*, 4043–4049.
- (20) Volpe, D.; Casado-Rivera, E.; Alden, L.; Lind, C.; Hagerdon, K.; Downie, C.; Korzeniewski, C.; DiSalvo, F. J.; Abruña, H. D. *J. Electrochem. Soc.* **2004**, *151*, A971–A977.
- (21) Liu, H.; Song, C.; Zhang, L.; Zhang, J.; Wang, H.; Wilkinson, D. *J. Power Sources* **2006**, *165*, 95–110.
- (22) He, C.; Desani, S.; Brown, G.; Bollepalli, S. *Electrochem. Soc. Interface* **2005**, *14*, 41–44.
- (23) Ball, S. C. *Platinum Met. Rev.* **2005**, *49*, 27–32.
- (24) Gasteiger, H. A.; Kocha, S. S.; Sompalli, B.; Wagner, F. T. *Appl. Catal., B* **2005**, *56*, 9–35.
- (25) Chiu, H. W.; Kauzlarich, S. M. *Chem. Mater.* **2006**, *18*, 1023–1028.
- (26) Chiu, H. W.; Chervin, C. N.; Kauzlarich, S. M. *Chem. Mater.* **2005**, *17*, 4845–4864.
- (27) Baldwin, R. K.; Pettigrew, K. A.; Ratai, E.; Augustine, M. P.; Kauzlarich, S. M. *Chem. Commun.* **2002**, 1822–1823.

- (28) Adam, W.; Arce, J. *J. Org. Chem.* **1972**, *37*, 507–508.

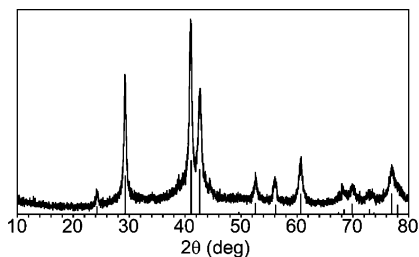


**Figure 1.** Powder X-ray diffraction pattern of PtPb nanoparticles prepared in THF at room temperature and exposed to air directly. Overlaid are the reported peak positions and intensities of PtPb. The mean crystal domain size is 16 nm as determined from the peak widths.

isopropyl alcohol, 20  $\mu$ L 5% w/w Nafion) were sonicated for 1 h. Intermetallic nanoparticle-coated glassy carbon electrodes were rotated at 2000 rpm during cyclic voltammetry experiments to determine electrocatalytic activity.

## Results

Dimethyl(1,5-cyclooctadiene)platinum and lead(II) 2-ethylhexanoate were selected as suitable metal-organic precursors for this synthesis because of their solubilities in the chosen solvents, because they are commercially available, and because they do not contain halides. Absorption of halides by the catalyst surface is known to degrade (“poison”) the catalytic activity of metallic nanoparticles during electrochemical testing.<sup>29</sup> The exclusion of halides from the reactions eliminates this possibility.

**PtPb Nanoparticles Prepared in THF.** The pXRD pattern of PtPb nanoparticles exposed to air directly matches the crystal structure of PtPb (Figure 1). No peaks corresponding to Pt, Pb, other intermetallics in the Pt–Pb system (Pt<sub>3</sub>Pb and PtPb<sub>4</sub>),<sup>30,31</sup> or any other Pb- or Pt-containing compounds (including oxides) are present in the diffraction pattern. This demonstrates that the desired intermetallic was successfully prepared. (Occasionally, peaks belonging to Pt<sub>3</sub>Pb, PtPb<sub>4</sub>, or NaPb<sub>2</sub>(CO<sub>3</sub>)<sub>2</sub>OH are present as minor impurities.) An average PtPb crystal domain size of 16 nm can be calculated from the Scherer equation.<sup>32</sup> SEM images of these samples show highly agglomerated PtPb nanocrystals (Figure 2a,b) with structure on the nanoscale clearly visible. Such agglomeration is expected since there are no surfactants or other stabilizers used in the synthetic procedure to prevent agglomeration. STEM images of these samples showed very similar results: PtPb nanocrystals of an average size consistent with what is measured from pXRD that are agglomerated into a random network of particles (Figure 3a,b). EDX analysis of single particles of 20–50 nm in diameter showed that Pt and Pb were both present in a 1:1 ratio ( $\pm$ 5%) in all particles measured. An oxygen signal is also present, suggesting the presence of a thin surface oxide on the particles. It is difficult to quantitatively evaluate the oxygen content because oxygen may also be present on the copper sample holder. No other elements were detectable

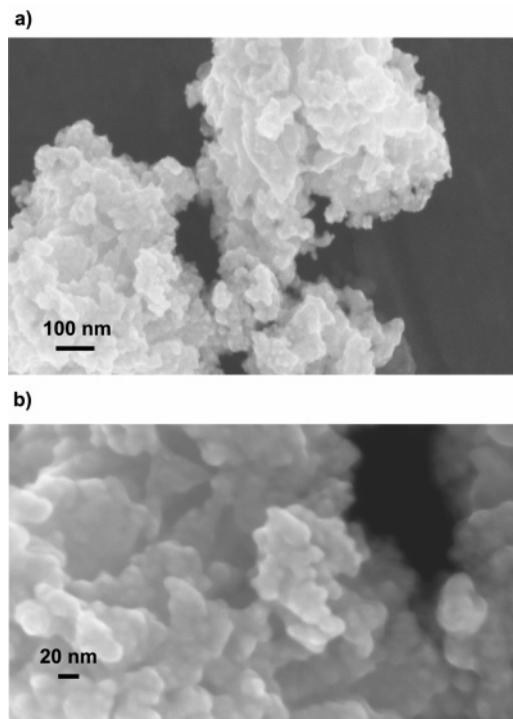


**Figure 2.** SEM images of the PtPb nanoparticles prepared in THF at room temperature and exposed to air directly. The images do not change significantly upon lengthy exposure to SEM beam.

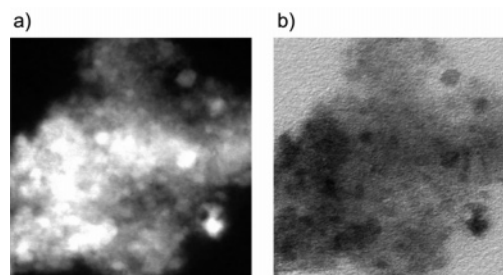


**Figure 3.** (a) Bright field and (b) dark field STEM images of PtPb nanoparticles prepared in THF at room temperature and exposed to air directly. Full scale = 63 nm.

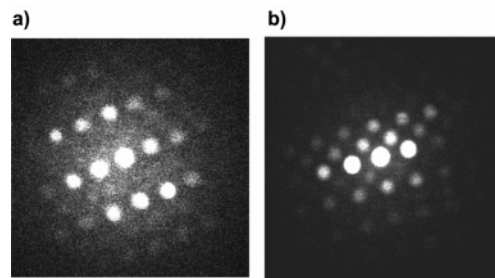


**Figure 4.** (a) and (b) CBED images of two PtPb nanoparticles (oriented in different crystallographic directions) prepared in THF at room temperature and exposed to air directly.

by EDX. CBED patterns further confirmed the single-crystal nature of each PtPb particle (Figure 4a,b). SEM images of these PtPb nanoparticles synthesized without sonicating the product in hexanes and ethanol show that a significant amount of hydrocarbon residues (possibly polymeric) coat the surface of the nanoparticles.

Further investigations revealed that the nature of the end product was very much dependent on the manner by which it was exposed to air after the washing process. Products

(29) Hubbard, A. T. *Chem. Rev.* **1988**, *88*, 633–656.

(30) Hansen, M. *Constitution of Binary Alloys*, 2nd ed.; McGraw Hill: New York, 1958.

(31) Doernickel, F. Z. *Anorg. Chem.* **1908**, *54*, 358–365.

(32) Warren, B. E. *X-ray Diffraction*, 1st ed.; Dover Publications Inc.: Mineola, NY, 1990.



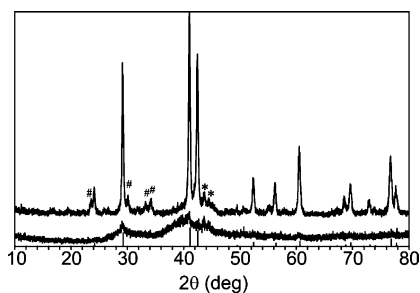


**Figure 5.** pXRD patterns of as-prepared Pt–Pb product prepared at room temperature in THF and exposed to air after backfilling with argon gas (lower) and again (upper) after annealing the product at 200 °C for 24 h. Overlaid are the reported peak positions and intensities for PtPb. #, unknown impurity peaks; \*, stainless steel sample holder.

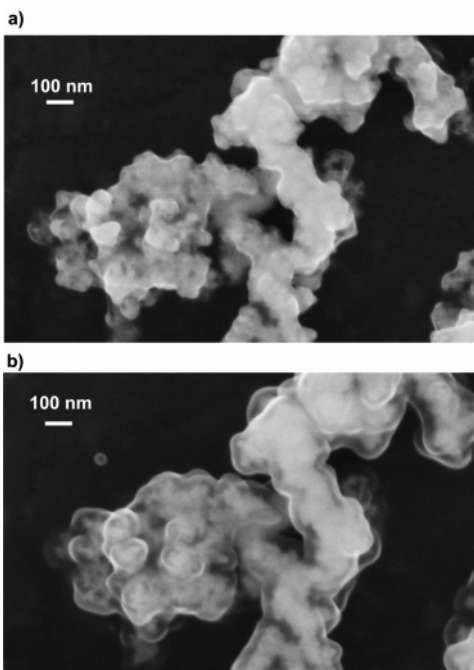


**Figure 6.** (a) SEM images of PtPb nanoparticles exposed to air slowly. (b) Image of the same area taken 3 min later. Note the formation of a transparent coating of hydrocarbons on the particles after only 3 min.

exposed to air by first backfilling with argon gas before opening the tube to air yielded pXRD patterns with low intensity and broad peaks, which approximately match the more intense peak positions of the PtPb structure (Figure 5), but since the peaks are broad, the presence of other phases cannot be discounted. Annealing the product, by sealing it in an evacuated quartz tube and heating at 200 °C for 24 h, shows PtPb intermetallic as the main crystalline phase by pXRD (Figure 5) with a mean crystal domain size of 30 nm. The impurity peaks in this pattern cannot be indexed to any likely impurity, but they may be related to the presence of hydrogen byproducts remaining in the sample (see below). SEM images of the as-prepared samples also show a high degree of agglomeration (Figure 6a). These agglomerates develop a smooth transparent coating under lengthy irradiation from the electron beam (Figure 6b). The formation of this coating is likely due to residual hydrocarbon byproducts still present in the agglomerate migrating to the particle surface, which are attracted to and cross-linked by the electron beam.<sup>33,34</sup> This is also observed in samples exposed to air directly, but only if they are *not* washed with hexanes

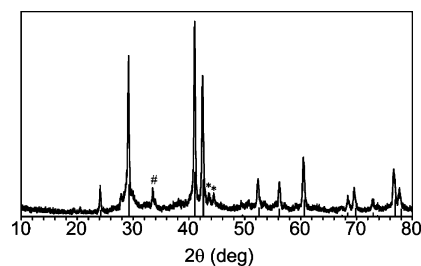


**Figure 7.** pXRD pattern of PtPb nanoparticles refluxed in diglyme for 2 h. Overlaid are the reported peak positions and intensities for PtPb. The mean crystal domain size is 32 nm as determined by peak widths. #, impurity (possibly PbO or PtPb<sub>4</sub>); \*, stainless steel sample holder.

and ethanol. Images of well-washed samples exposed to air directly do not change significantly upon prolonged irradiation of the SEM electron beam and do not develop the coating seen in samples exposed to air after backfilling with argon gas. Any residual hydrocarbons in such samples are most likely removed during their pyrophoric reaction with air.

Since bulk PtPb is fully oxidized to Pt and PbO by heating in air to 500 °C, it is expected that a thin oxide layer should form on the surface of the reaction product when exposed to air. In fact, XPS experiments on PtPb bulk show that the surface is oxidized to a depth of ~1 nm.<sup>35</sup> A thin surface oxide formation explains the temperature increase and white smoke observed when the product is exposed to air quickly. This air sensitivity cannot be due to leftover sodium naphthalide since any unreacted sodium naphthalide is quenched during the ethanol wash. Thus, we are confident that the as-formed product is not phase-separated into different phases or compositions on length scales of 5 nm or more, but there are no analytical tools available that can detect such separation on the scale of 1–2 nm. Apparently, in the samples exposed to air directly, the released heat that results from rapid surface oxidation is enough to promote the grain growth of PtPb intermetallic. The surface oxide(s) formed must be very poorly crystalline or be less than 5% of the product mass since no X-ray peaks can be ascribed to these phases.

**PtPb Nanoparticles Prepared in Diglyme.** Attempts were made to controllably induce crystallinity into the as-formed product by refluxing the THF solution (bp = 65 °C) prior to workup, but this had no observable effect. Therefore, diglyme (bp = 162 °C) was chosen as a replacement solvent because of its similarities to THF in terms of, e.g., solubility of reactants. Performing the reduction at room temperature and then refluxing the solution, even for the briefest amount of time, yielded products whose pXRD patterns showed sharp PtPb peaks, even after being exposed to air slowly after backfilling with argon gas (Figure 7). Calculated mean crystal domain sizes increased some with increasing refluxing time

- (33) Reimer, L. *Scanning Electron Microscopy: Physics of Image Formation and Microanalysis*, 2nd ed.; Springer: New York, 1998; pp 132–134.
- (34) Goldstein, J.; Newbury, D.; Joy, D.; Lyman, C.; Echlin, P.; Lifshin, E.; Sawyer, L.; Michael, J. *Scanning Electron Microscopy and X-ray Microanalysis*, 3rd ed.; Kluwer Academic/Plenum Publishers: Dordrecht, The Netherlands, 2003; p 203.
- (35) Blasini, D. R.; Rochefort, D.; Fachini, E.; Alden, L. R.; DiSalvo, F. J.; Cabrera, C. R.; Abruña, H. D. *Surf. Sci.* **2006**, *600*, 2670–2680.

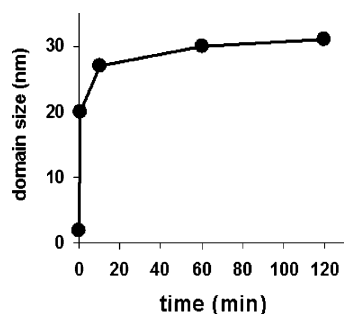


**Figure 8.** Domain size of PtPb nanocrystals refluxed for different times in diglyme (bp = 162 °C).

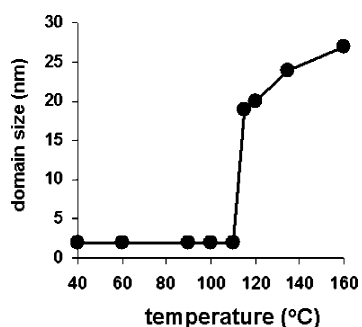


**Figure 9.** Domain size of PtPb nanocrystals heated in diglyme at different temperatures for 10 min.

(Figure 8), growing quickly up to 27 nm within the first 10 min and then slowly thereafter. Since 10 min of heating was enough time to induce good crystallinity at the boiling point of diglyme, syntheses were carried out with 10 min of heating at different temperatures to determine the effect of temperature on inducing crystallinity (Figure 9). The onset of crystal domain growth is sharp and occurs above 110 °C. SEM images of these samples show highly agglomerated PtPb nanocrystals with structure on the nanoscale clearly visible (Figure 10).

This sharp onset in crystallinity is suggestive of a nucleation phenomenon, rather than a diffusion-controlled process, indicating that the as-formed product is made up of very small ( $\leq 2$  nm) Pt–Pb nanocrystalites that can easily be induced to form single-crystalline nanoparticles of PtPb intermetallic roughly an order of magnitude larger in size. Since the pXRD pattern of the as-formed product is so broad, we cannot be certain that this initial product consists of pure PtPb, or perhaps is a heterogeneous mixture of nanocrystals containing the two elements in different ratios, although the centroid positions of the broad peaks are closer to those expected for PtPb than any other Pt–Pb phases. Such a phenomenon would not be entirely surprising as size dependencies for the formation of nanoparticles have been reported for other bimetallic systems.<sup>36–39</sup> Thermodynamic instabilities can arise on the nanoscale when the surface free energy of the material begins to prevail over the bulk free energy of formation. Therefore, there may be critical domain

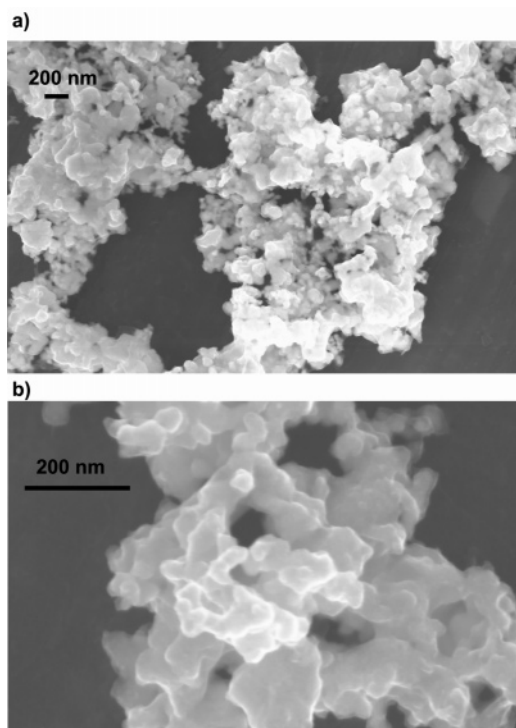


**Figure 10.** SEM images of PtPb nanoparticles refluxed in diglyme for 2 h at different magnifications at (a) lower magnification and (b) higher magnification.

sizes below which ordered PtPb intermetallic nanoparticles are thermodynamically unstable. At this point, since no analytical tools can probe the homogeneity of agglomerates on the scale of 1–2 nm, we can only speculate as to the true nature of the as-formed product.  $\text{Pb}_5\text{O}_8$  formation has been observed (by pXRD) in several samples that initially had broad peaks and low intensity when they are stored in air over several months. This has not been observed in any of the PtPb samples with domain sizes an order of magnitude larger.

pXRD patterns of some of the samples annealed in diglyme were taken prior to exposure to air, followed by a quick exposure to air (peeling the mylar covering off the sample holder) and a second pXRD measurement. One sample heated to 120 °C for 10 min produced a small amount of white smoke when exposed to air, but the pXRD pattern changed very little, and the crystal domain size calculated from the Scherer equation slightly increased to 21 nm from 20 nm, but this is likely within expected margins of error. Several samples that were heated to temperatures  $< 110$  °C showed a much greater reaction upon exposure to air. In those cases, the pXRD patterns prior to rapid air exposure had low intensity and broad peaks and afterward had pXRD patterns with PtPb domain sizes around 30 nm.

**Electrocatalytic Oxidation of Formic Acid.** Cyclic voltammetry in solutions containing 0.5 M formic acid and 0.1 M sulfuric acid was performed on glassy carbon electrodes coated with suspensions prepared from some of the PtPb samples. A typical cyclic voltammogram is presented as Figure 11. The results of all samples tested are presented in Table 1. A commercial PtRu alloy catalyst (4 nm, supported on Vulcan XC-72R, E-TEK) was also tested for comparison. While there is some variation between

(36) Yasuda, H.; Mori, H.; Furuya, K. *Philos. Mag. Lett.* **2000**, *80*, 181–186.

(37) Yasuda, H.; Mitsuishi, K.; Mori, H. *Phys. Rev. B* **2001**, *64*, 094101–09106.

(38) Lee, J. G.; Mori, H.; Yasuda, H. *Phys. Rev. B* **2002**, *65*, 1321061–1321064.

(39) Yasuda, H.; Mori, H. *Ann. Phys.* **1997**, *22*, C2.

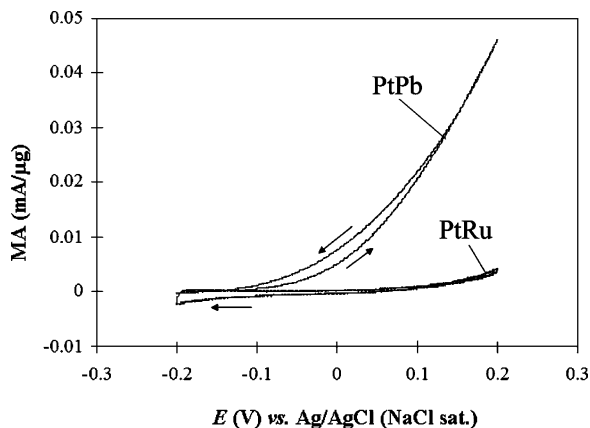


**Figure 11.** Cyclic voltammograms of PtPb nanoparticles (135 °C in diglyme for 10 min, crystal domain size 24 nm) and PtRu nanoparticles (4 nm, supported on Vulcan XC-72R) in 0.5 M formic acid, 0.1 M H<sub>2</sub>SO<sub>4</sub> at electrode rotation rate of 2000 rpm and 10 mV/s. Catalyst loading was 70 μg/cm<sup>2</sup>.

**Table 1. Onset Potentials and Mass Activities Obtained by Cyclic Voltammetry in 0.5 M Formic Acid, 0.1 M H<sub>2</sub>SO<sub>4</sub> of PtPb Nanoparticles (70 μg/cm<sup>2</sup>) Heated in Diglyme<sup>a</sup>**

domain size	preparation method	onset potential	mass activity at 0.2 V (vs Ag/AgCl)
32 nm	reflux <sup>b</sup> 2 h	-100 mV	9.2 μA/μg
29 nm	reflux <sup>b</sup> 1 h	-80 mV	13 μA/μg
27 nm	reflux <sup>b</sup> 10 min	-120 mV	21 μA/μg
20 nm	reflux <sup>b</sup> 5 s	-170 mV	37 μA/μg
24 nm	135 °C, 10 min	-150 mV	45 μA/μg
22 nm	120 °C, 10 min	-130 mV	24 μA/μg
PtRu (4 nm), supported on Vulcan XC-72R	-	+150 mV	0.5 μA/μg

<sup>a</sup> Electrode rotation rate and potential scan rate were 2000 rpm and 10 mV/s, respectively. <sup>b</sup> bp of diglyme = 162 °C.

samples, all show onset potentials and mass activities superior to the commercial PtRu catalyst and have similar onset potentials to values previously reported for bulk PtPb.<sup>19</sup> In general, the best results came from samples heated to higher temperatures for shorter amounts of time. The variability between samples may not be surprising as we have shown previously that the electrochemical activity of PtPb in bulk is somewhat sensitive to surface treatments.<sup>20</sup> In this case, the variability may be a result of the highly agglomerated nature of nanoparticles as well as varying amounts of

surface oxidation and residual hydrocarbons. Indeed, that these samples show such remarkable activity toward formic acid oxidation despite those potential faults is noteworthy. Additionally, it is worth pointing out that the commercial PtRu nanoparticles are smaller (4 nm) and unagglomerated (supported on carbon black). Unfortunately, these PtPb nanoparticle samples were too small (typically less than 40 mg) to reliably measure their surface areas by BET, but it is undeniable that their catalytic surface areas are less than the commercial PtRu to which they are compared. That they nevertheless produce mass activities 20–100 times higher at relatively low potentials is striking. These results suggest that PtPb nanoparticles may be a superior anode catalyst to what is currently used in formic acid fuel cells.

## Conclusions

In this paper, we demonstrated that PtPb nanoparticles can be successfully synthesized by chemically co-reducing dimethyl(1,5-cyclooctadiene)platinum and lead(II) 2-ethylhexanoate with sodium naphthalide and subsequently heating the product above 110 °C. This compound was targeted for synthesis based on the assumption that it may be an interesting material for direct fuel cell electrocatalysis. Electrochemical evaluation of these samples shows that nanoscale PtPb, even agglomerated, is superior to commercial PtRu catalyst for formic acid oxidation. Efforts to perfect this synthesis for optimized electrocatalytic activity,<sup>40</sup> characterize the catalytic surface, and also prepare other intermetallic compounds by this method are currently underway.

**Acknowledgment.** This work was supported by the Basic Energy Sciences Division of the Department of Energy through Grant No. DE – FG02 87ER45298. The authors would like to thank Mick Thomas for help with the SEM, STEM, and CBED images and the EDX data. This work made use of the Keck SEM facility and the UHV-STEM Laboratory of the Cornell Center for Materials Research (CCMR) with support from the National Science Foundation Materials Research Science and Engineering Centers (MRSEC) program Grant No. DMR 05204040.

CM060927J

(40) Alden, L. R.; Roychowdhury, C.; Matsumoto, F.; Han, D. K.; Zeldovich, V. B.; Abruña, H. D.; DiSalvo, F. J. *Langmuir*, in press.